https://doi.org/10.15302/frontphys.2025.024205

RESEARCH ARTICLE

Anyonic topological flat bands

Xiaoqi Zhou, Weixuan Zhang†, Xiangdong Zhang‡

Key Laboratory of advanced optoelectronic quantum architecture and measurements of Ministry of Education,
Beijing Key Laboratory of Nanophotonics & Ultrafine Optoelectronic Systems,
School of Physics, Beijing Institute of Technology, Beijing 100081, China
Corresponding authors. E-mail: †zhangwx@bit.edu.cn, ‡zhangxd@bit.edu.cn
Received August 24, 2024; accepted October 21, 2024

Supporting Information

Note 1. Eigen-equations of the two-anyon model

In this part, we derive the eigen-equation of two anyons in the proposed lattice model. Here, $C_{(m,\alpha)(n,\beta)}$ is the probability amplitude with one anyon at 'α' sublattice in the mth unit and the other one at 'β' sublattice in the nth unit. Solving the Schrödinger equation, we can obtain the eigen-equation with respect to $C_{(m,\alpha)(n,\beta)}$ as

$$\begin{aligned}\varepsilon C_{(m,A)(n,A)} =& -J(e^{i\theta(\delta_{m,n}+\delta_{m+1,n})}C_{(m,A)(n-1,A)} + e^{-i\theta(\delta_{m,n}+\delta_{m-1,n})}C_{(m,A)(n+1,A)} + C_{(m-1,A)(n,A)} \\ &+C_{(m+1,A)(n,A)} + C_{(m,B)(n,A)} + e^{-i\theta(\delta_{m,n}+\delta_{m-1,n})}C_{(m,A)(n,B)} \\ &+C_{(m-1,B)(n,A)} + e^{i\theta(\delta_{m,n}+\delta_{m+1,n})}C_{(m,A)(n-1,B)}) \\ &-P\delta_{mn}(C_{(m,B)(n,B)} + C_{(m-1,B)(n-1,B)}) + U\delta_{mn}C_{(m,A)(n,A)} + V\delta_{m(n\pm1)}C_{(m,A)(n,A)},\end{aligned} \tag{S1}$$

$$\begin{aligned}\varepsilon C_{(m,A)(n,B)} =& -J(C_{(m,A)(n-1,B)} + C_{(m,A)(n+1,B)} + C_{(m-1,A)(n,B)} + C_{(m+1,A)(n,B)} \\ &+e^{i\theta(\delta_{m,n}+\delta_{m+1,n})}C_{(m,A)(n,A)} + C_{(m,B)(n,B)} + C_{(m+1,A)(n,A)} + C_{(m,B)(n-1,B)}),\end{aligned} \tag{S2}$$

$$\begin{aligned}\varepsilon C_{(m,B)(n,A)} =& -J(C_{(m,B)(n-1,A)} + C_{(m,B)(n+1,A)} + C_{(m-1,B)(n,A)} + C_{(m+1,B)(n,A)} \\ &+C_{(m,A)(n,A)} + e^{-i\theta(\delta_{m,n}+\delta_{m-1,n})}C_{(m,B)(n,B)} + C_{(m-1,B)(n,B)} + C_{(m,A)(n-1,A)}),\end{aligned} \tag{S3}$$

$$\begin{aligned}\varepsilon C_{(m,B)(n,B)} =& -J(e^{i\theta(\delta_{m,n}+\delta_{m+1,n})}C_{(m,B)(n-1,B)} + e^{-i\theta(\delta_{m,n}+\delta_{m-1,n})}C_{(m,B)(n+1,B)} \\ &+C_{(m-1,B)(n,B)} + C_{(m+1,B)(n,B)} + e^{i\theta(\delta_{m,n}+\delta_{m+1,n})}C_{(m,B)(n,A)} + C_{(m,A)(n,B)} \\ &+e^{-i\theta(\delta_{m,n}+\delta_{m-1,n})}C_{(m+1,B)(n,A)} + C_{(m,A)(n+1,B)}) \\ &-P\delta_{mn}(C_{(m,A)(n,A)} + C_{(m+1,A)(n+1,A)}) + U\delta_{mn}C_{(m,B)(n,B)}.\end{aligned} \tag{S4}$$

Under the case with strong interactions of two anyons ($U, V \gg J$), the probability amplitude $C_{(m,\alpha)(n,\beta)}$ of two-anyon states without interaction can be deleted in the steady-state Schrödinger equation of two anyons with strong interaction ($C_{(n,A)(n,A)}$, $C_{(n+1,A)(n,A)}$, $C_{(n,A)(n+1,A)}$ and $C_{(n,B)(n,B)}$) in the high-energy region ($\varepsilon \sim U, V$). In this case, we can obtain effective eigenequations of two strongly interacting anyon in the high-energy region ($\varepsilon \sim U, V$) as

$$\begin{aligned}\varepsilon C_{(n,A)(n,A)} =& -J[e^{i\theta}C_{(n,A)(n-1,A)} + e^{-i\theta}C_{(n,A)(n+1,A)} + C_{(n-1,A)(n,A)} + C_{(n+1,A)(n,A)}] \\ &-P[C_{(n,B)(n,B)} + C_{(n-1,B)(n-1,B)}] + UC_{(n,A)(n,A)},\end{aligned} \tag{S5}$$

$$\varepsilon C_{(n+1,A)(n,A)} = -J[e^{-i\theta}C_{(n+1,A)(n+1,A)} + C_{(n,A)(n,A)}] + VC_{(n+1,A)(n,A)}, \tag{S6}$$

$$\varepsilon C_{(n,A)(n+1,A)} = -J[e^{i\theta}C_{(n,A)(n,A)} + C_{(n+1,A)(n+1,A)}] + VC_{(n,A)(n+1,A)}, \tag{S7}$$

$$\varepsilon C_{(n,B)(n,B)} = -P\left[C_{(n,A)(n,A)} + C_{(n+1,A)(n+1,A)}\right] + UC_{(n,B)(n,B)}, \tag{S8}$$

where the deleted terms of two-anyon states without interactions are highlighted by strikethroughs.

Note 2. Numerical results of anyonic eigenspectra with different interaction strengths

In this part, we investigate the influence of the interaction strength on the energy spectra of the two-anyon model. Figs. S1(a)-(c) present the numerical results of eigenspectra of two anyons with the interaction strength being (*U*=*V*=20), (*U*=*V*=20), and (*U*=*V*=20), respectively. It is clearly shown that the flatness of two-anyon flat bands is significantly enhanced with the interaction strength being increased. When the interaction strength is infinite, the strictly degenerate eigenenergies of flat bands appear.

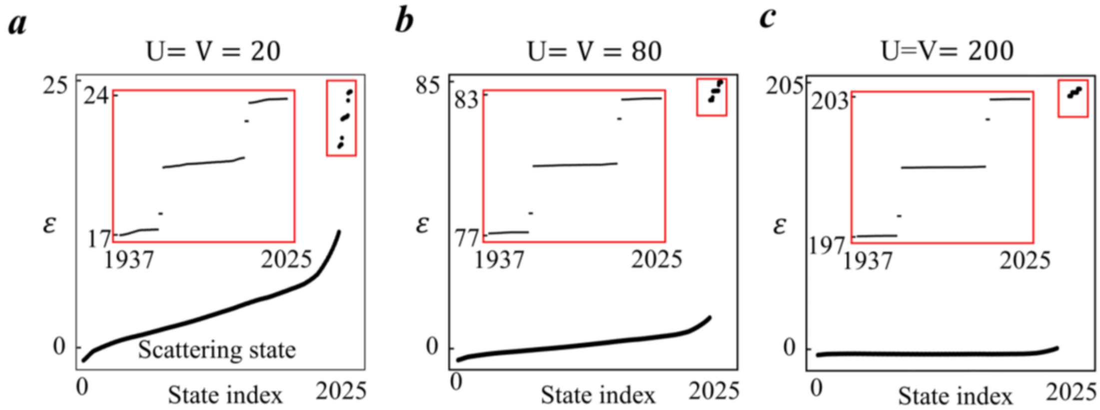

Fig. S1 (a-c) Numerical results of eigenspectra with the interaction strength being (*U*=*V*=20), (*U*=*V*=80), and (*U*=*V*=200), respectively.

Note3. Numerical results of anyonic flat bands with different statistical angles

In this part, we give numerical results two-anyon eigen-spectra with different statistical angles, where the completely topological flat bands of two strongly-interacted anyons appear. Based on the effective Hamiltonian of two strongly-interacted anyons in the momentum space [Eq. (3) in the main text], it is deduced that the perfect two-anyon flat bands can be obtained with J, P and θ satisfying the relationship of $2J^2cos(\theta) + P^2 = 0$. To verify the correctness of this formalism, as shown in Figs. S2(a)-(c), we calculate eigenspectra of two anyons with the statistical angle being $\theta = 2/3\pi$, $3/4\pi$ and $4/5\pi$, where the associated hopping strengths equal to $P = 2.467$, $P = 2.171$, and $P = 2.242$, respectively. And, we set the single-particle hopping strength as $J = 1$. Enlarged views correspond to eigen-spectra of two anyons with strong interaction. We can see that completely flat bands appear in two-anyon systems with different statistical angles, being consistent with the analytical prediction.

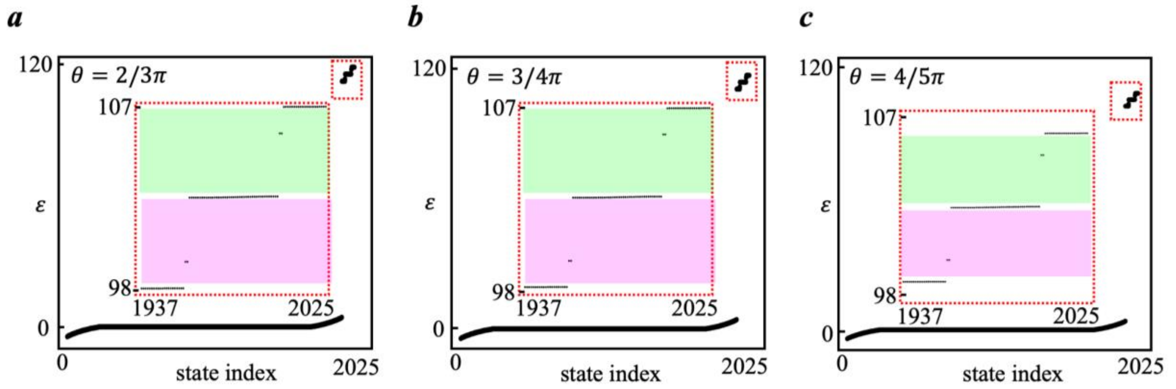

Fig. S2 (a-c) The eigenspectra of two-anyon systems with the statistical angle being $\theta = 2/3\pi$, $3/4\pi$ and $4/5\pi$, respectively. The two-anyon direct hopping strengths equal to $P = 2.467$, $P = 2.171$, and $P = 2.242$. Enlarged views of eigenspectra of two strongly interacting anyons are shown in right insets.

Note 4. The square-root topological insulator induced by quantum statistics

Here, we discuss the square-root topological insulator induced by quantum statistics. We note that the eigen-spectrum of $H(k)$ with $\theta = \pi$ has a two-fold degenerated subspace at zero energy, and two non-degenerated bands at energies $\pm 2\sqrt{2}$. The topology of two non-degenerated bands can be evaluated by the Abelian Zak's phase as

$$\gamma_i = i \int_{\pi}^{-\pi} dk \langle \nu_i(k) | \partial_k | \nu_i(k) \rangle. \tag{S9}$$

Differently, in order to capture the topological property of degenerated energy bands, the generalization of Abelian Zak's phase, called as the Wilzcek-Zee phase, should be used. It is expressed as

$$\gamma = \int_{-k}^{k} Tr[A(k)]dk, \tag{S10}$$

where we have $A(k)^{nm} = \langle \nu_n(k) | \partial_k | \nu_m(k) \rangle$ with two labels of 'n' and 'm' running over the involved energy bands.

To get the topological invariant, we firstly derivate the analytical solution of two-anyon bulk bands $|\nu_i(k)\rangle$ ($i = 1,2,3,4$) of the effective k-space Hamiltonian $H(k)$. They are expressed as

$$|\nu_1\rangle = \frac{1}{2}\begin{pmatrix} -2\sqrt{2}e^{ik} \\ 1 - e^{ik} \\ \sqrt{2}(1 - e^{ik}) \\ -1 + e^{ik} \end{pmatrix}, \; |\nu_2\rangle = \frac{1}{2\sqrt{2}}\begin{pmatrix} 0 \\ 1 \\ 0 \\ 1 \end{pmatrix}, \; |\nu_3\rangle = \frac{1}{2}\begin{pmatrix} 0 \\ -\sqrt{2}(1 + e^{ik}) \\ -1 + e^{ik} \\ 0 \end{pmatrix}, \; |\nu_4\rangle = \frac{1}{2}\begin{pmatrix} 2\sqrt{2}e^{ik} \\ 1 - e^{ik} \\ \sqrt{2}(1 + e^{ik}) \\ -1 + e^{ik} \end{pmatrix}. \tag{S11}$$

Using Supplementary Eqs. (a9)-(a11), the topological invariants of different energy bands are obtained. Specifically, the Zak's phase of the isolated energy band at energy $E_1 = -2\sqrt{2}$ ($E_4 = 2\sqrt{2}$) equals to $\gamma_1 = \frac{\pi}{2}$ ($\gamma_4 = \frac{\pi}{2}$), and the Wilzcek-Zee phase of degenerated zero modes spanned by $|\nu_2\rangle$ and $|\nu_3\rangle$ equals to $\gamma_{2,3} = \pi$. It is clearly shown that the winding phases γ_1 and γ_4 of lowest and highest energy bands are not quantized.

Then, we discuss the bulk topological properties of the square of k-space Hamiltonian $H^2(k)$, which is written as

$$H^2(k) = \begin{pmatrix} 8 & 0 & 0 & 0 \\ 0 & 2-2cosk & -2i\sqrt{2}sink & -2+2cosk \\ 0 & 2i\sqrt{2}sink & 4+4cosk & -2i\sqrt{2}sink \\ 0 & -2+2cosk & 2i\sqrt{2}sink & 2-2cosk \end{pmatrix}. \tag{S12}$$

In this case, four eigen-vectors of $H^2(k)$ can be derived in the compact form as

$$|w_1\rangle = \frac{1}{2\sqrt{2}}\begin{pmatrix} 0 \\ 1 \\ 0 \\ 1 \end{pmatrix},\ |w_2\rangle = \frac{1}{\sqrt{2}}\begin{pmatrix} 0 \\ -\sqrt{2}(1+e^{ik}) \\ -1+e^{ik} \\ 0 \end{pmatrix},\ |w_3\rangle = \frac{1}{\sqrt{2}}\begin{pmatrix} 0 \\ 1-e^{ik} \\ \sqrt{2}(1+e^{ik}) \\ -1+e^{ik} \end{pmatrix},\ |w_4\rangle = \begin{pmatrix} 1 \\ 0 \\ 0 \\ 0 \end{pmatrix}. \tag{S13}$$

We note that the state of $|w_1\rangle$ is degenerated with $|w_2\rangle$ at *E*=0, and the state of $|w_3\rangle$ is degenerated with $|w_4\rangle$ at *E*=8. In this case, we can calculate the Wilzcek-Zee phases of these two types of degenerated eigen-bands. The Wilzcek-Zee phase of the degenerate subspace spanned by $|w_1\rangle$ and $|w_2\rangle$ equals to $\gamma_{1,2} = \pi$. And, the Wilzcek-Zee of the degenerated subspace spanned by $|w_3\rangle$ and $|w_4\rangle$ equals to $\gamma_{3,4} = -\pi$. Those quantized topological invariants clearly manifest the topological feature of the effective two-anyon model.

To further propose a clear explanation of topological properties for the two-anyon mode, we perform a basis transformation of $H^2(k)$. The corresponding rotation matrix is expressed as

$$R = e^{-i\begin{pmatrix} 0 & 0 & 0 & 0 \\ 0 & 0 & 0 & -i \\ 0 & 0 & 0 & 0 \\ 0 & i & 0 & 0 \end{pmatrix}\frac{\pi}{4}} e^{-i\begin{pmatrix} 0 & 0 & 0 & 0 \\ 0 & 0 & -i & 0 \\ 0 & i & 0 & 0 \\ 0 & 0 & 0 & 0 \end{pmatrix}\frac{\pi}{4}}. \tag{S14}$$

After the basis transformation, the resulting Hamiltonian is in the form of

$$H_{trans}^2(k) = \begin{pmatrix} 8 & 0 & 0 & 0 \\ 0 & 4 & -4e^{ik} & 0 \\ 0 & -4e^{-ik} & 4 & 0 \\ 0 & 0 & 0 & 0 \end{pmatrix}. \tag{S15}$$

It is clearly shown that $H_{trans}^2(k)$ can be decomposed by a 1D SSH model and two isolated sub-lattice sites with onsite potentials being 0 and 8. Hence, the non-trivial topology of 1D SSH chain can leads to the existence of topological boundary states of the effective two-anyon model.

Note 5. Details for the derivation of circuit eigen-equation with $\theta = \pi$

In this part, we give a detailed derivation of circuit eigen-equation, which could be mapped to the 1D stationary Schrödinger equation of two pseudofermions. Here, each lattice site possesses two circuit nodes. In this case, the voltage and current at the site $(m,\alpha),(n,\alpha)$ should be written as $V_{(m,\alpha)(n,\beta)} = [V_{1,(m,\alpha)(n,\beta)},\ V_{2,(m,\alpha)(n,\beta)}]^T$ and $I_{(m,\alpha)(n,\beta)} = [I_{1,(m,\alpha)(n,\beta)},\ I_{2,(m,\alpha)(n,\beta)}]^T$. In addition, the voltage on the circuit node $(m,\alpha),(n,\beta)$ is in the form of $V_{j,(m,\alpha)(n,\beta)}e^{i\omega t}$ (*j*=1 and 2).

At first, we focus on the circuit node located at the main diagonal line $(n,\alpha),(n,\alpha)$. Carrying out the Kirchhoff's law on the circuit node pair at $(n,A),(n,A)$, $(n,A),(n,B)$, $(n,B),(n,A)$, and $(n,B),(n,B)$, we get the following equations as

$$\begin{vmatrix} I_{1,(n,A)(n,A)} \\ I_{2,(n,A)(n,A)} \end{vmatrix} = i\omega C\begin{vmatrix} 1 & -1 \\ -1 & 1 \end{vmatrix}\begin{vmatrix} V_{1,(n,A)(n,A)} \\ V_{2,(n,A)(n,A)} \end{vmatrix} + i\omega C(\begin{vmatrix} V_{1,(n,A)(n,A)} - V_{1,(n+1,A)(n,A)} \\ V_{2,(n,A)(n,A)} - V_{2,(n+1,A)(n,A)} \end{vmatrix} + \begin{vmatrix} V_{1,(n,A)(n,A)} - V_{1,(n-1,A)(n,A)} \\ V_{2,(n,A)(n,A)} - V_{2,(n-1,A)(n,A)} \end{vmatrix}$$

$$+\begin{vmatrix} V_{1,(n,A)(n,A)} - V_{1,(n,B)(n,A)} \\ V_{2,(n,A)(n,A)} - V_{2,(n,B)(n,A)} \end{vmatrix} + \begin{vmatrix} V_{1,(n,A)(n,A)} - V_{1,(n-1,B)(n,A)} \\ V_{2,(n,A)(n,A)} - V_{2,(n-1,B)(n,A)} \end{vmatrix} + \begin{vmatrix} V_{1,(n,A)(n,A)} - V_{2,(n,A)(n+1,A)} \\ V_{2,(n,A)(n,A)} - V_{1,(n,A)(n+1,A)} \end{vmatrix}$$

$$+\begin{vmatrix} V_{1,(n,A)(n,A)} - V_{2,(n,A)(n-1,A)} \\ V_{2,(n,A)(n,A)} - V_{1,(n,A)(n-1,A)} \end{vmatrix} + \begin{vmatrix} V_{1,(n,A)(n,A)} - V_{2,(n,A)(n,B)} \\ V_{2,(n,A)(n,A)} - V_{1,(n,A)(n,B)} \end{vmatrix} + \begin{vmatrix} V_{1,(n,A)(n,A)} - V_{2,(n,A)(n-1,B)} \\ V_{2,(n,A)(n,A)} - V_{1,(n,A)(n-1,B)} \end{vmatrix})$$

$$+i\omega C_P(\begin{vmatrix} V_{1,(n,A)(n,A)} - V_{1,(n,B)(n,B)} \\ V_{2,(n,A)(n,A)} - V_{2,(n,B)(n,B)} \end{vmatrix} + \begin{vmatrix} V_{1,(n,A)(n,A)} - V_{1,(n-1,B)(n-1,B)} \\ V_{2,(n,A)(n,A)} - V_{2,(n-1,B)(n-1,B)} \end{vmatrix}) + \frac{1}{i\omega L}\begin{vmatrix} V_{1,(n,A)(n,A)} \\ V_{2,(n,A)(n,A)} \end{vmatrix} + i\omega C_U \begin{vmatrix} V_{1,(n,A)(n,A)} \\ V_{2,(n,A)(n,A)} \end{vmatrix},$$

(S16)

$$\begin{vmatrix} I_{1,(n,A)(n,B)} \\ I_{2,(n,A)(n,B)} \end{vmatrix} = i\omega C \begin{vmatrix} 1 & -1 \\ -1 & 1 \end{vmatrix} \begin{vmatrix} V_{1,(n,A)(n,B)} \\ V_{2,(n,A)(n,B)} \end{vmatrix} + i\omega C(\begin{vmatrix} V_{1,(n,A)(n,B)} - V_{1,(n+1,A)(n,B)} \\ V_{2,(n,A)(n,B)} - V_{2,(n+1,A)(n,B)} \end{vmatrix} + \begin{vmatrix} V_{1,(n,A)(n,B)} - V_{1,(n-1,A)(n,B)} \\ V_{2,(n,A)(n,B)} - V_{2,(n-1,A)(n,B)} \end{vmatrix}$$

$$+\begin{vmatrix} V_{1,(n,A)(n,B)} - V_{1,(n,B)(n,B)} \\ V_{2,(n,A)(n,B)} - V_{2,(n,B)(n,B)} \end{vmatrix} + \begin{vmatrix} V_{1,(n,A)(n,B)} - V_{1,(n-1,B)(n,B)} \\ V_{2,(n,A)(n,B)} - V_{2,(n-1,B)(n,B)} \end{vmatrix} + \begin{vmatrix} V_{1,(n,A)(n,B)} - V_{2,(n,A)(n,A)} \\ V_{2,(n,A)(n,B)} - V_{1,(n,A)(n,A)} \end{vmatrix}$$

$$+\begin{vmatrix} V_{1,(n,A)(n,B)} - V_{1,(n,A)(n-1,B)} \\ V_{2,(n,A)(n,B)} - V_{2,(n,A)(n-1,B)} \end{vmatrix} + \begin{vmatrix} V_{1,(n,A)(n,B)} - V_{1,(n,A)(n+1,A)} \\ V_{2,(n,A)(n,B)} - V_{2,(n,A)(n+1,A)} \end{vmatrix} + \begin{vmatrix} V_{1,(n,A)(n,B)} - V_{1,(n,A)(n+1,B)} \\ V_{2,(n,A)(n,B)} - V_{2,(n,A)(n+1,B)} \end{vmatrix}) - \frac{i}{\omega L}\begin{vmatrix} V_{1,(n,A)(n,B)} \\ V_{2,(n,A)(n,B)} \end{vmatrix},$$

(S17)

$$\begin{vmatrix} I_{1,(n,B)(n,A)} \\ I_{2,(n,B)(n,A)} \end{vmatrix} = i\omega C \begin{vmatrix} 1 & -1 \\ -1 & 1 \end{vmatrix} \begin{vmatrix} V_{1,(n,B)(n,A)} \\ V_{2,(n,B)(n,A)} \end{vmatrix} + i\omega C(\begin{vmatrix} V_{1,(n,B)(n,A)} - V_{1,(n+1,A)(n,A)} \\ V_{2,(n,B)(n,A)} - V_{2,(n+1,A)(n,A)} \end{vmatrix} + \begin{vmatrix} V_{1,(n,B)(n,A)} - V_{1,(n+1,B)(n,A)} \\ V_{2,(n,B)(n,A)} - V_{2,(n+1,B)(n,A)} \end{vmatrix}$$

$$+\begin{vmatrix} V_{1,(n,B)(n,A)} - V_{1,(n,A)(n,A)} \\ V_{2,(n,B)(n,A)} - V_{2,(n,A)(n,A)} \end{vmatrix} + \begin{vmatrix} V_{1,(n,B)(n,A)} - V_{1,(n-1,B)(n,A)} \\ V_{2,(n,B)(n,A)} - V_{2,(n-1,B)(n,A)} \end{vmatrix} + \begin{vmatrix} V_{1,(n,B)(n,A)} - V_{2,(n,B)(n,B)} \\ V_{2,(n,B)(n,A)} - V_{2,(n,B)(n,B)} \end{vmatrix}$$

$$+\begin{vmatrix} V_{1,(n,B)(n,A)} - V_{1,(n,B)(n+1,A)} \\ V_{2,(n,B)(n,A)} - V_{2,(n,B)(n+1,A)} \end{vmatrix} + \begin{vmatrix} V_{1,(n,B)(n,A)} - V_{1,(n,B)(n-1,A)} \\ V_{2,(n,B)(n,A)} - V_{2,(n,B)(n-1,A)} \end{vmatrix} + \begin{vmatrix} V_{1,(n,B)(n,A)} - V_{1,(n,B)(n-1,B)} \\ V_{2,(n,B)(n,A)} - V_{2,(n,B)(n-1,B)} \end{vmatrix}) + \frac{1}{i\omega L}\begin{vmatrix} V_{1,(n,B)(n,A)} \\ V_{2,(n,B)(n,A)} \end{vmatrix}$$

(S18)

$$\begin{vmatrix} I_{1,(n,B)(n,B)} \\ I_{2,(n,B)(n,B)} \end{vmatrix} = i\omega C \begin{vmatrix} 1 & -1 \\ -1 & 1 \end{vmatrix} \begin{vmatrix} V_{1,(n,B)(n,B)} \\ V_{2,(n,B)(n,B)} \end{vmatrix} + i\omega C(\begin{vmatrix} V_{1,(n,B)(n,B)} - V_{1,(n+1,A)(n,B)} \\ V_{2,(n,B)(n,B)} - V_{2,(n+1,A)(n,B)} \end{vmatrix} + \begin{vmatrix} V_{1,(n,B)(n,B)} - V_{1,(n+1,B)(n,B)} \\ V_{2,(n,B)(n,B)} - V_{2,(n+1,B)(n,B)} \end{vmatrix}$$

$$+\begin{vmatrix} V_{1,(n,B)(n,B)} - V_{1,(n,A)(n,B)} \\ V_{2,(n,B)(n,B)} - V_{2,(n,A)(n,B)} \end{vmatrix} + \begin{vmatrix} V_{1,(n,B)(n,B)} - V_{1,(n-1,B)(n,B)} \\ V_{2,(n,B)(n,B)} - V_{2,(n-1,B)(n,B)} \end{vmatrix} + \begin{vmatrix} V_{1,(n,B)(n,B)} - V_{2,(n,B)(n+1,A)} \\ V_{2,(n,B)(n,B)} - V_{1,(n,B)(n+1,A)} \end{vmatrix}$$

$$+\begin{vmatrix} V_{1,(n,B)(n,B)} - V_{2,(n,B)(n+1,B)} \\ V_{2,(n,B)(n,B)} - V_{1,(n,B)(n+1,B)} \end{vmatrix} + \begin{vmatrix} V_{1,(n,B)(n,B)} - V_{2,(n,B)(n,A)} \\ V_{2,(n,B)(n,B)} - V_{1,(n,B)(n,A)} \end{vmatrix} + \begin{vmatrix} V_{1,(n,B)(n,B)} - V_{2,(n,B)(n-1,B)} \\ V_{2,(n,B)(n,B)} - V_{1,(n,B)(n-1,B)} \end{vmatrix}$$

$$+\frac{1}{i\omega L}\begin{vmatrix} V_{1,(n,B)(n,B)} \\ V_{2,(n,B)(n,B)} \end{vmatrix} + i\omega C_U \begin{vmatrix} V_{1,(n,B)(n,B)} \\ V_{2,(n,B)(n,B)} \end{vmatrix}) + i\omega C_P(\begin{vmatrix} V_{1,(n,B)(n,B)} - V_{1,(n,A)(n,A)} \\ V_{2,(n,B)(n,B)} - V_{2,(n,A)(n,A)} \end{vmatrix} + \begin{vmatrix} V_{1,(n,B)(n,B)} - V_{1,(n+1,A)(n+1,A)} \\ V_{2,(n,B)(n,B)} - V_{2,(n+1,A)(n+1,A)} \end{vmatrix}),$$

(S19)

where L is the inductor linking the node $(n,\alpha)(n,\beta)$ to the ground. C and C_P are the capacitances used for connecting circuit nodes along the *m or n*-axis and the diagonal line. C_U is the capacitance linking the circuit nodes belonging to the same lattice site. We assume that there is no external source, so that the current flowing out of the node is zero. In this case, Supplementary Eqs. (S16)-(S19) become

$$\frac{1}{i\omega L}\begin{vmatrix} V_{1,(n,A)(n,A)} \\ V_{2,(n,A)(n,A)} \end{vmatrix} = (C_U + 8C + 2C_P)\begin{vmatrix} V_{1,(n,A)(n,A)} \\ V_{2,(n,A)(n,A)} \end{vmatrix} + C\begin{vmatrix} 1 & -1 \\ -1 & 1 \end{vmatrix}\begin{vmatrix} V_{1,(n,A)(n,A)} \\ V_{2,(n,A)(n,A)} \end{vmatrix} - C\begin{vmatrix} 0 & 1 \\ 1 & 0 \end{vmatrix}(\begin{vmatrix} V_{1,(n,A)(n+1,A)} \\ V_{2,(n,A)(n+1,A)} \end{vmatrix}$$

$$+\begin{vmatrix} V_{1,(n,A)(n-1,A)} \\ V_{2,(n,A)(n-1,A)} \end{vmatrix} + \begin{vmatrix} V_{1,(n,A)(n,B)} \\ V_{2,(n,A)(n,B)} \end{vmatrix} + \begin{vmatrix} V_{1,(n,A)(n-1,B)} \\ V_{2,(n,A)(n-1,B)} \end{vmatrix}) - C(\begin{vmatrix} V_{1,(n+1,A)(n,A)} \\ V_{2,(n+1,A)(n,A)} \end{vmatrix} + \begin{vmatrix} V_{1,(n-1,A)(n,A)} \\ V_{2,(n-1,A)(n,A)} \end{vmatrix}$$

$$+\begin{vmatrix} V_{1,(n,B)(n,A)} \\ V_{2,(n,B)(n,A)} \end{vmatrix} + \begin{vmatrix} V_{1,(n-1,B)(n,A)} \\ V_{2,(n-1,B)(n,A)} \end{vmatrix}) - C_P\begin{vmatrix} V_{1,(n,B)(n,B)} \\ V_{2,(n,B)(n,B)} \end{vmatrix} - C_P\begin{vmatrix} V_{1,(n-1,B)(n-1,B)} \\ V_{2,(n-1,B)(n-1,B)} \end{vmatrix}, \tag{S20}$$

$$\frac{1}{i\omega L}\begin{vmatrix} V_{1,(n,A)(n,B)} \\ V_{2,(n,A)(n,B)} \end{vmatrix} = 8C\begin{vmatrix} V_{1,(n,A)(n,B)} \\ V_{2,(n,A)(n,B)} \end{vmatrix} + C\begin{vmatrix} 1 & -1 \\ -1 & 1 \end{vmatrix}\begin{vmatrix} V_{1,(n,A)(n,B)} \\ V_{2,(n,A)(n,B)} \end{vmatrix} - C(\begin{vmatrix} V_{1,(n+1,A)(n,B)} \\ V_{2,(n+1,A)(n,B)} \end{vmatrix} + \begin{vmatrix} V_{1,(n-1,A)(n,B)} \\ V_{2,(n-1,A)(n,B)} \end{vmatrix}$$

$$+\begin{vmatrix} V_{1,(n,B)(n,B)} \\ V_{2,(n,B)(n,B)} \end{vmatrix} + \begin{vmatrix} V_{1,(n-1,B)(n,B)} \\ V_{2,(n-1,B)(n,B)} \end{vmatrix} + \begin{vmatrix} V_{1,(n,A)(n-1,B)} \\ V_{2,(n,A)(n-1,B)} \end{vmatrix} + \begin{vmatrix} V_{1,(n,A)(n+1,A)} \\ V_{2,(n,A)(n+1,A)} \end{vmatrix} + \begin{vmatrix} V_{1,(n,A)(n+1,B)} \\ V_{2,(n,A)(n+1,B)} \end{vmatrix}) - C\begin{vmatrix} 0 & 1 \\ 1 & 0 \end{vmatrix}\begin{vmatrix} V_{1,(n,A)(n,A)} \\ V_{2,(n,A)(n,A)} \end{vmatrix}$$

(S21)

$$\frac{1}{i\omega L}\begin{vmatrix}V_{1,(n,B)(n,A)}\\V_{2,(n,B)(n,A)}\end{vmatrix} = 8C\begin{vmatrix}V_{1,(n,B)(n,A)}\\V_{2,(n,B)(n,A)}\end{vmatrix} + C\begin{vmatrix}1 & -1\\-1 & 1\end{vmatrix}\begin{vmatrix}V_{1,(n,B)(n,A)}\\V_{2,(n,B)(n,A)}\end{vmatrix} - C(\begin{vmatrix}V_{1,(n+1,A)(n,A)}\\V_{2,(n+1,A)(n,A)}\end{vmatrix} + \begin{vmatrix}V_{1,(n+1,B)(n,A)}\\V_{2,(n+1,B)(n,A)}\end{vmatrix}$$

$$+\begin{vmatrix}V_{1,(n,A)(n,A)}\\V_{2,(n,A)(n,A)}\end{vmatrix} + \begin{vmatrix}V_{1,(n-1,B)(n,A)}\\V_{2,(n-1,B)(n,A)}\end{vmatrix} + \begin{vmatrix}V_{1,(n,B)(n+1,A)}\\V_{2,(n,B)(n+1,A)}\end{vmatrix} + \begin{vmatrix}V_{1,(n,B)(n-1,A)}\\V_{2,(n,B)(n-1,A)}\end{vmatrix} + \begin{vmatrix}V_{1,(n,B)(n-1,B)}\\V_{2,(n,B)(n-1,B)}\end{vmatrix}) - C\begin{vmatrix}0 & 1\\1 & 0\end{vmatrix}\begin{vmatrix}V_{1,(n,B)(n,B)}\\V_{2,(n,B)(n,B)}\end{vmatrix}, \quad \text{(S22)}$$

$$\frac{1}{i\omega L}\begin{vmatrix}V_{1,(n,B)(n,B)}\\V_{2,(n,B)(n,B)}\end{vmatrix} = (C_U + 8C + 2C_P)\begin{vmatrix}V_{1,(n,B)(n,B)}\\V_{2,(n,B)(n,B)}\end{vmatrix} + C\begin{vmatrix}1 & -1\\-1 & 1\end{vmatrix}\begin{vmatrix}V_{1,(n,B)(n,B)}\\V_{2,(n,B)(n,B)}\end{vmatrix} - C\begin{vmatrix}0 & 1\\1 & 0\end{vmatrix}(\begin{vmatrix}V_{1,(n,B)(n+1,A)}\\V_{2,(n,B)(n+1,A)}\end{vmatrix}$$

$$+\begin{vmatrix}V_{1,(n,B)(n+1,B)}\\V_{2,(n,B)(n+1,B)}\end{vmatrix} + \begin{vmatrix}V_{1,(n,B)(n,A)}\\V_{2,(n,B)(n,A)}\end{vmatrix} + \begin{vmatrix}V_{1,(n,B)(n-1,B)}\\V_{2,(n,B)(n-1,B)}\end{vmatrix}) - C(\begin{vmatrix}V_{1,(n+1,A)(n,B)}\\V_{2,(n+1,A)(n,B)}\end{vmatrix} + \begin{vmatrix}V_{1,(n+1,B)(n,B)}\\V_{2,(n+1,B)(n,B)}\end{vmatrix} + \begin{vmatrix}V_{1,(n,A)(n,B)}\\V_{2,(n,A)(n,B)}\end{vmatrix}$$

$$+\begin{vmatrix}V_{1,(n-1,B)(n,B)}\\V_{2,(n-1,B)(n,B)}\end{vmatrix}) + \frac{1}{i\omega L}\begin{vmatrix}V_{1,(n,B)(n,B)}\\V_{2,(n,B)(n,B)}\end{vmatrix} + i\omega C_U\begin{vmatrix}V_{1,(n,B)(n,B)}\\V_{2,(n,B)(n,B)}\end{vmatrix} - C_P\left(\begin{vmatrix}V_{1,(n,A)(n,A)}\\V_{2,(n,A)(n,A)}\end{vmatrix} + \begin{vmatrix}V_{1,(n+1,A)(n+1,A)}\\V_{2,(n+1,A)(n+1,A)}\end{vmatrix}\right). \quad \text{(S23)}$$

Performing the diagonalization of Supplementary Eqs. (S21)-(S24) with a unitary transformation

$$F = \frac{1}{\sqrt{2}}\begin{bmatrix}1 & e^{i\pi}\\1 & -e^{i\pi}\end{bmatrix}, \quad \text{(S24)}$$

Supplementary Eqs. (S20)-(S23) become

$$-C\begin{vmatrix}0 & 0\\0 & 2\end{vmatrix}\begin{vmatrix}V_{\uparrow,(n,A)(n,A)}\\V_{\downarrow,(n,A)(n,A)}\end{vmatrix} = (C_U + 8C + 2C_P)\begin{vmatrix}V_{\uparrow,(n,A)(n,A)}\\V_{\downarrow,(n,A)(n,A)}\end{vmatrix} - \frac{1}{i\omega L}\begin{vmatrix}V_{\uparrow,(n,A)(n,A)}\\V_{\downarrow,(n,A)(n,A)}\end{vmatrix} - C\begin{vmatrix}1 & 0\\0 & e^{-i\pi}\end{vmatrix}(\begin{vmatrix}V_{\uparrow,(n,A)(n+1,A)}\\V_{\downarrow,(n,A)(n+1,A)}\end{vmatrix}$$

$$+\begin{vmatrix}V_{\uparrow,(n,A)(n,B)}\\V_{\downarrow,(n,A)(n,B)}\end{vmatrix}) - C\begin{vmatrix}1 & 0\\0 & e^{i\pi}\end{vmatrix}(\begin{vmatrix}V_{\uparrow,(n,A)(n-1,A)}\\V_{\downarrow,(n,A)(n-1,A)}\end{vmatrix} + \begin{vmatrix}V_{\uparrow,(n,A)(n-1,B)}\\V_{\downarrow,(n,A)(n-1,B)}\end{vmatrix}) - C(\begin{vmatrix}V_{\uparrow,(n+1,A)(n,A)}\\V_{\downarrow,(n+1,A)(n,A)}\end{vmatrix} + \begin{vmatrix}V_{\uparrow,(n-1,A)(n,A)}\\V_{\downarrow,(n-1,A)(n,A)}\end{vmatrix}$$

$$+\begin{vmatrix}V_{\uparrow,(n,B)(n,A)}\\V_{\downarrow,(n,B)(n,A)}\end{vmatrix} + \begin{vmatrix}V_{\uparrow,(n-1,B)(n,A)}\\V_{\downarrow,(n-1,B)(n,A)}\end{vmatrix}) - C_P(\begin{vmatrix}V_{\uparrow,(n,B)(n,B)}\\V_{\downarrow,(n,B)(n,B)}\end{vmatrix} + \begin{vmatrix}V_{\uparrow,(n-1,B)(n-1,B)}\\V_{\downarrow,(n-1,B)(n-1,B)}\end{vmatrix}), \quad \text{(S25)}$$

$$-C\begin{vmatrix}0 & 0\\0 & 2\end{vmatrix}\begin{vmatrix}V_{\uparrow,(n,A)(n,B)}\\V_{\downarrow,(n,A)(n,B)}\end{vmatrix} = 8C\begin{vmatrix}V_{\uparrow,(n,A)(n,B)}\\V_{\downarrow,(n,A)(n,B)}\end{vmatrix} - \frac{1}{i\omega L}\begin{vmatrix}V_{\uparrow,(n,A)(n,B)}\\V_{\downarrow,(n,A)(n,B)}\end{vmatrix} - C\begin{vmatrix}1 & 0\\0 & e^{i\pi}\end{vmatrix}\begin{vmatrix}V_{\uparrow,(n,A)(n,A)}\\V_{\downarrow,(n,A)(n,A)}\end{vmatrix}$$

$$-C(\begin{vmatrix}V_{\uparrow,(n+1,A)(n,B)}\\V_{\downarrow,(n+1,A)(n,B)}\end{vmatrix} + \begin{vmatrix}V_{\uparrow,(n-1,A)(n,B)}\\V_{\downarrow,(n-1,A)(n,B)}\end{vmatrix} + \begin{vmatrix}V_{\uparrow,(n,B)(n,B)}\\V_{\downarrow,(n,B)(n,B)}\end{vmatrix} + \begin{vmatrix}V_{\uparrow,(n-1,B)(n,B)}\\V_{\downarrow,(n-1,B)(n,B)}\end{vmatrix} + \begin{vmatrix}V_{\uparrow,(n,A)(n-1,B)}\\V_{\downarrow,(n,A)(n-1,B)}\end{vmatrix}$$

$$+\begin{vmatrix}V_{\uparrow,(n,A)(n+1,A)}\\V_{\downarrow,(n,A)(n+1,A)}\end{vmatrix} + \begin{vmatrix}V_{\uparrow,(n,A)(n+1,B)}\\V_{\downarrow,(n,A)(n+1,B)}\end{vmatrix}), \quad \text{(S26)}$$

$$-C\begin{vmatrix}0 & 0\\0 & 2\end{vmatrix}\begin{vmatrix}V_{\uparrow,(n,B)(n,A)}\\V_{\downarrow,(n,B)(n,A)}\end{vmatrix} = 8C\begin{vmatrix}V_{\uparrow,(n,B)(n,A)}\\V_{\downarrow,(n,B)(n,A)}\end{vmatrix} - \frac{1}{i\omega L}\begin{vmatrix}V_{\uparrow,(n,B)(n,A)}\\V_{\downarrow,(n,B)(n,A)}\end{vmatrix} - C\begin{vmatrix}1 & 0\\0 & e^{-i\pi}\end{vmatrix}\begin{vmatrix}V_{\uparrow,(n,B)(n,B)}\\V_{\downarrow,(n,B)(n,B)}\end{vmatrix}$$

$$-C(\begin{vmatrix}V_{\uparrow,(n+1,A)(n,A)}\\V_{\downarrow,(n+1,A)(n,A)}\end{vmatrix} + \begin{vmatrix}V_{\uparrow,(n+1,B)(n,A)}\\V_{\downarrow,(n+1,B)(n,A)}\end{vmatrix} + \begin{vmatrix}V_{\uparrow,(n,A)(n,A)}\\V_{\downarrow,(n,A)(n,A)}\end{vmatrix} + \begin{vmatrix}V_{\uparrow,(n-1,B)(n,A)}\\V_{\downarrow,(n-1,B)(n,A)}\end{vmatrix} + \begin{vmatrix}V_{\uparrow,(n,B)(n+1,A)}\\V_{\downarrow,(n,B)(n+1,A)}\end{vmatrix}$$

$$+\begin{vmatrix}V_{\uparrow,(n,B)(n-1,A)}\\V_{\downarrow,(n,B)(n-1,A)}\end{vmatrix} + \begin{vmatrix}V_{\uparrow,(n,B)(n-1,B)}\\V_{\downarrow,(n,B)(n-1,B)}\end{vmatrix}), \quad \text{(S27)}$$

$$-C\begin{vmatrix}0 & 0\\0 & 2\end{vmatrix}\begin{vmatrix}V_{\uparrow,(n,B)(n,B)}\\V_{\downarrow,(n,B)(n,B)}\end{vmatrix} = (C_U + 8C + 2C_P)\begin{vmatrix}V_{\uparrow,(n,B)(n,B)}\\V_{\downarrow,(n,B)(n,B)}\end{vmatrix} - \frac{1}{i\omega L}\begin{vmatrix}V_{\uparrow,(n,B)(n,B)}\\V_{\downarrow,(n,B)(n,B)}\end{vmatrix} - C\begin{vmatrix}1 & 0\\0 & e^{-i\pi}\end{vmatrix}(\begin{vmatrix}V_{\uparrow,(n,B)(n+1,A)}\\V_{\downarrow,(n,B)(n+1,A)}\end{vmatrix}$$

$$+\begin{vmatrix}V_{\uparrow,(n,B)(n+1,B)}\\V_{\downarrow,(n,B)(n+1,B)}\end{vmatrix}) - C\begin{vmatrix}1 & 0\\0 & e^{i\pi}\end{vmatrix}(\begin{vmatrix}V_{\uparrow,(n,B)(n,A)}\\V_{\downarrow,(n,B)(n,A)}\end{vmatrix} + \begin{vmatrix}V_{\uparrow,(n,B)(n-1,B)}\\V_{\downarrow,(n,B)(n-1,B)}\end{vmatrix})$$

$$-C(\begin{vmatrix}V_{\uparrow,(n+1,A)(n,B)}\\V_{\downarrow,(n+1,A)(n,B)}\end{vmatrix} + \begin{vmatrix}V_{\uparrow,(n+1,B)(n,B)}\\V_{\downarrow,(n+1,B)(n,B)}\end{vmatrix} + \begin{vmatrix}V_{\uparrow,(n,A)(n,B)}\\V_{\downarrow,(n,A)(n,B)}\end{vmatrix} + \begin{vmatrix}V_{\uparrow,(n-1,B)(n,B)}\\V_{\downarrow,(n-1,B)(n,B)}\end{vmatrix})$$

$$-C_P\begin{vmatrix}V_{\uparrow,(n,A)(n,A)}\\V_{\downarrow,(n,A)(n,A)}\end{vmatrix} - C_P\begin{vmatrix}V_{\uparrow,(n+1,A)(n+1,A)}\\V_{\downarrow,(n+1,A)(n+1,A)}\end{vmatrix}. \quad \text{(S28)}$$

The basis are expressed as $V_{\uparrow(\downarrow),(m,\alpha)(n,\beta)} = F[V_{1,(m,\alpha)(n,\beta)}, V_{2,(m,\alpha)(n,\beta)}]^T$, which are two decoupled terms acting as a pair of pseudospins $V_{\uparrow,(m,\alpha)(n,\beta)} = (V_{1,(m,\alpha)(n,\beta)} + V_{2,(m,\alpha)(n,\beta)})/\sqrt{2}$ and $V_{\downarrow,(m,\alpha)(n,\beta)} = (V_{1,(m,\alpha)(n,\beta)} - V_{2,(m,\alpha)(n,\beta)})/\sqrt{2}$. Thus, Supplementary Eqs. (a25)-(a28) can be divided into two independent equations as

$$0=(C_U+8C+2C_P)\,V_{\uparrow,(n,A)(n,A)}-\frac{1}{i\omega L}V_{\uparrow,(n,A)(n,A)}-C(V_{\uparrow,(n,A)(n+1,A)}+V_{\uparrow,(n,A)(n-1,A)}+V_{\uparrow,(n+1,A)(n,A)}$$
$$+V_{\uparrow,(n-1,A)(n,A)}+V_{\uparrow,(n,A)(n,B)}+V_{\uparrow,(n,A)(n-1,B)}+V_{\uparrow,(n,B)(n,A)}+V_{\uparrow,(n-1,B)(n,A)})$$
$$-C_P(V_{\uparrow,(n,B)(n,B)}+V_{\uparrow,(n-1,B)(n-1,B)}), \tag{S29}$$

$$(\frac{1}{i\omega L}-2C)V_{\downarrow,(n,A)(n,A)}=(C_U+8C+2C_P)V_{\downarrow,(n,A)(n,A)}-\frac{1}{i\omega L}V_{\downarrow,(n,A)(n,A)}-C(e^{-i\pi}V_{\downarrow,(n,A)(n+1,A)}$$
$$+e^{-i\pi}V_{\downarrow,(n,A)(n,B)}+e^{i\pi}V_{\downarrow,(n,A)(n-1,A)}+e^{i\pi}V_{\downarrow,(n,A)(n-1,B)}+V_{\downarrow,(n,B)(n,A)}+V_{\downarrow,(n-1,B)(n,A)})$$
$$+V_{\downarrow,(n+1,A)(n,A)}+V_{\downarrow,(n-1,A)(n,A)})-\ C_P(V_{\downarrow,(n,B)(n,B)}+V_{\downarrow,(n-1,B)(n-1,B)}), \tag{S30}$$

$$0=8CV_{\uparrow,(n,A)(n,B)}-\frac{1}{i\omega L}V_{\uparrow,(n,A)(n,B)}-C(V_{\uparrow,(n,A)(n,A)}+V_{\uparrow,(n+1,A)(n,B)}+V_{\uparrow,(n-1,A)(n,B)}+V_{\uparrow,(n,B)(n,B)}$$
$$+V_{\uparrow,(n-1,B)(n,B)}+V_{\uparrow,(n,A)(n-1,B)}+V_{\uparrow,(n,A)(n+1,A)}+V_{\uparrow,(n,A)(n+1,B)}, \tag{S31}$$

$$(\frac{1}{i\omega L}-2C)\,V_{\downarrow,(n,A)(n,B)}=8CV_{\downarrow,(n,A)(n,B)}-\frac{1}{i\omega L}V_{\downarrow,(n,A)(n,B)}-C(e^{i\pi}V_{\downarrow,(n,A)(n,A)}+V_{\downarrow,(n+1,A)(n,B)}$$
$$+V_{\downarrow,(n-1,A)(n,B)}+V_{\downarrow,(n,B)(n,B)}+V_{\downarrow,(n-1,B)(n,B)}+V_{\downarrow,(n,A)(n-1,B)}+V_{\downarrow,(n,A)(n+1,A)}+V_{\downarrow,(n,A)(n+1,B)}), \tag{S32}$$

$$0=8CV_{\uparrow,(n,B)(n,A)}-\frac{1}{i\omega L}V_{\uparrow,(n,B)(n,A)}-C(V_{\uparrow,(n,B)(n,B)}+V_{\uparrow,(n+1,A)(n,A)}+V_{\uparrow,(n+1,B)(n,A)}+V_{\uparrow,(n,A)(n,A)}$$
$$+V_{\uparrow,(n-1,B)(n,A)}+V_{\uparrow,(n,B)(n+1,A)}+V_{\uparrow,(n,B)(n-1,A)}+V_{\uparrow,(n,B)(n-1,B)}), \tag{S33}$$

$$(\frac{1}{i\omega L}-2C)\,V_{\downarrow,(n,B)(n,A)}=8CV_{\downarrow,(n,B)(n,A)}-\frac{1}{i\omega L}V_{\downarrow,(n,B)(n,A)}-C(e^{-i\pi}V_{\downarrow,(n,B)(n,B)}+V_{\downarrow,(n+1,A)(n,A)}+V_{\downarrow,(n+1,B)(n,A)}$$
$$+V_{\downarrow,(n,A)(n,A)}+V_{\downarrow,(n-1,B)(n,A)}+V_{\downarrow,(n,B)(n+1,A)}+V_{\downarrow,(n,B)(n-1,A)}+V_{\downarrow,(n,B)(n-1,B)}), \tag{S34}$$

$$0=(C_U+8C+2C_P)V_{\uparrow,(n,B)(n,B)}-\frac{1}{i\omega L}V_{\uparrow,(n,B)(n,B)}-C(V_{\uparrow,(n,B)(n+1,A)}+V_{\uparrow,(n,B)(n+1,B)}+V_{\uparrow,(n,B)(n,A)}$$
$$+V_{\uparrow,(n,B)(n-1,B)}+V_{\uparrow,(n+1,A)(n,B)}+V_{\uparrow,(n+1,B)(n,B)}+V_{\uparrow,(n,A)(n,B)}+V_{\uparrow,(n-1,B)(n,B)})$$
$$-C_P(V_{\uparrow,(n,A)(n,A)}+V_{\uparrow,(n+1,A)(n+1,A)}), \tag{S35}$$

$$\left(\frac{1}{i\omega L}-2C\right)V_{\downarrow,(n,B)(n,B)}=(C_U+8C+2C_P)V_{\downarrow,(n,B)(n,B)}-C(e^{-i\pi}V_{\downarrow,(n,B)(n+1,A)}$$
$$+e^{-i\pi}V_{\downarrow,(n,B)(n+1,B)}+e^{i\pi}V_{\downarrow,(n,B)(n,A)}+e^{i\pi}V_{\downarrow,(n,B)(n-1,B)}+V_{\downarrow,(n+1,A)(n,B)}+V_{\downarrow,(n+1,B)(n,B)}+V_{\downarrow,(n,A)(n,B)}$$
$$+V_{\downarrow,(n-1,B)(n,B)})-C_P(V_{\downarrow,(n,A)(n,A)}+V_{\downarrow,(n+1,A)(n+1,A)}). \tag{S36}$$

Based on the similar derivations, we can obtain the eigen-equation at any circuit node $(m,\alpha),(n,\beta)$. As for the case of $n=m-1$, we have

$$\left(\frac{1}{i\omega L}-2C\right)V_{\downarrow,(n,A)(n-1,A)}=(C_V+8C)V_{\downarrow,(n,A)(n-1,A)}-\frac{1}{i\omega L}V_{\downarrow,(n,A)(n-1,A)}$$
$$-C(e^{i\pi}V_{\downarrow,(n,A)(n,A)}+V_{\downarrow,(n,A)(n-1,B)}+V_{\downarrow,(n,A)(n-2,A)}+V_{\downarrow,(n,A)(n-2,B)}$$
$$+V_{\downarrow,(n,B)(n-1,A)}+V_{\downarrow,(n-1,B)(n-1,A)})+V_{\downarrow,(n+1,A)(n-1,A)}+V_{\downarrow,(n-1,A)(n-1,A)}), \tag{S37}$$

$$(\frac{1}{i\omega L}-2C)\,V_{\downarrow,(n,A)(n-1,B)}=8CV_{\downarrow,(n,A)(n-1,B)}-\frac{1}{i\omega L}V_{\downarrow,(n,A)(n,B)}-C(V_{\downarrow,(n,A)(n-1,A)}+V_{\downarrow,(n+1,A)(n-1,B)}$$
$$+V_{\downarrow,(n-1,A)(n-1,B)}+V_{\downarrow,(n,B)(n-1,B)}+V_{\downarrow,(n-1,B)(n-1,B)}$$
$$+V_{\downarrow,(n,A)(n-2,B)}+e^{-i\pi}V_{\downarrow,(n,A)(n,A)}+V_{\downarrow,(n,A)(n,B)}), \tag{S38}$$

$$(\frac{1}{i\omega L}-2C)\,V_{\downarrow,(n,B)(n-1,A)}=8CV_{\downarrow,(n,B)(n,A)}-\frac{1}{i\omega L}V_{\downarrow,(n,B)(n,A)}-C(V_{\downarrow,(n,B)(n-1,B)}+V_{\downarrow,(n+1,A)(n-1,A)}$$

$$+V_{\downarrow,(n+1,B)(n-1,A)} + V_{\downarrow,(n,A)(n-1,A)} + V_{\downarrow,(n-1,B)(n-1,A)}$$

$$+V_{\downarrow,(n,B)(n,A)} + V_{\downarrow,(n,B)(n-2,A)} + V_{\downarrow,(n,B)(n-2,B)}), \tag{S39}$$

$$\left(\frac{1}{i\omega L} - 2C\right) V_{\downarrow,(n,B)(n-1,B)} = (C_U + 8C + 2C_P) V_{\downarrow,(n,B)(n-1,B)} - C(V_{\downarrow,(n,B)(n,A)} + e^{-i\pi} V_{\downarrow,(n,B)(n,B)}$$

$$+V_{\downarrow,(n,B)(n-1,A)} + V_{\downarrow,(n,B)(n-2,B)} + V_{\downarrow,(n+1,A)(n-1,B)} + V_{\downarrow,(n+1,B)(n-1,B)} + V_{\downarrow,(n,A)(n-1,B)} + V_{\downarrow,(n-1,B)(n-1,B)}). \tag{S40}$$

As for the case of $n = m + 1$, we have

$$\left(\frac{1}{i\omega L} - 2C\right) V_{\downarrow,(n,A)(n+1,A)} = (C_V + 8C) V_{\downarrow,(n,A)(n+1,A)} - \frac{1}{i\omega L} V_{\downarrow,(n,A)(n+1,A)}$$

$$-C(V_{\downarrow,(n,A)(n+2,A)} + V_{\downarrow,(n,A)(n+2,B)} + e^{i\pi} V_{\downarrow,(n,A)(n,A)} + V_{\downarrow,(n,A)(n,B)} + V_{\downarrow,(n,B)(n+1,A)} + V_{\downarrow,(n-1,B)(n+1,A)})$$

$$+V_{\downarrow,(n+1,A)(n+1,A)} + V_{\downarrow,(n-1,A)(n+1,A)})), \tag{S41}$$

$$(\frac{1}{i\omega L} - 2C)\, V_{\downarrow,(n,A)(n+1,B)} = 8C V_{\downarrow,(n,A)(n+1,B)} - \frac{1}{i\omega L} V_{\downarrow,(n,A)(n+1,B)} - C(V_{\downarrow,(n,A)(n+1,A)} + V_{\downarrow,(n+1,A)(n+1,B)}$$

$$+V_{\downarrow,(n-1,A)(n+1,B)} + V_{\downarrow,(n,B)(n+1,B)} + V_{\downarrow,(n-1,B)(n+1,B)} + V_{\downarrow,(n,A)(n,B)} + V_{\downarrow,(n,A)(n,A)} + V_{\downarrow,(n,A)(n,B)}), \tag{S42}$$

$$(\frac{1}{i\omega L} - 2C)\, V_{\downarrow,(n,B)(n+1,A)} = 8C V_{\downarrow,(n,B)(n+1,A)} - \frac{1}{i\omega L} V_{\downarrow,(n,B)(n+1,A)} - C(V_{\downarrow,(n,B)(n+1,B)} + V_{\downarrow,(n+1,A)(n+1,A)}$$

$$+V_{\downarrow,(n+1,B)(n+1,A)} + V_{\downarrow,(n,A)(n+1,A)} + V_{\downarrow,(n-1,B)(n+1,A)} + V_{\downarrow,(n,B)(n+2,A)} + V_{\downarrow,(n,B)(n,A)} + V_{\downarrow,(n,B)(n,B)}), \tag{S43}$$

$$\left(\frac{1}{i\omega L} - 2C\right) V_{\downarrow,(n,B)(n+1,B)} = (8C) V_{\downarrow,(n,B)(n+1,B)} - C(V_{\downarrow,(n,B)(n+2,A)} + V_{\downarrow,(n,B)(n+2,B)}$$

$$+V_{\downarrow,(n,B)(n+1,A)} + e^{i\pi} V_{\downarrow,(n,B)(n,B)} + V_{\downarrow,(n+1,A)(n+1,B)} + V_{\downarrow,(n+1,B)(n+1,B)} + V_{\downarrow,(n,A)(n+1,B)} + V_{\downarrow,(n-1,B)(n+1,B)}). \tag{S44}$$

As for the case of $|n - m| > 1$, we have

$$(\frac{1}{i\omega L} - 2C) V_{\downarrow,(m,A)(n,A)} = 8C V_{\downarrow,(m,A)(n,A)} - \frac{1}{i\omega L} V_{\downarrow,(m,A)(n,A)} - C(V_{\downarrow,(m,A)(n+1,A)} + V_{\downarrow,(m,A)(n,B)}$$

$$+V_{\downarrow,(m,A)(n-1,A)} + V_{\downarrow,(m,A)(n-1,B)} + V_{\downarrow,(m,B)(n,A)} + V_{\downarrow,(m-1,B)(n,A)}), \tag{S45}$$

$$(\frac{1}{i\omega L} - 2C)\, V_{\downarrow,(m,A)(n,B)} = 8C V_{\downarrow,(m,A)(n,B)} - \frac{1}{i\omega L} V_{\downarrow,(m,A)(n,B)} - C(V_{\downarrow,(m,A)(n,A)} + V_{\downarrow,(m+1,A)(n,B)}$$

$$+V_{\downarrow,(m-1,A)(n,B)} + V_{\downarrow,(m,B)(n,B)} + V_{\downarrow,(m-1,B)(n,B)} + V_{\downarrow,(m,A)(n-1,B)} + V_{\downarrow,(m,A)(n+1,A)} + V_{\downarrow,(m,A)(n+1,B)}), \tag{S46}$$

$$(\frac{1}{i\omega L} - 2C)\, V_{\downarrow,(m,B)(n,A)} = 8C V_{\downarrow,(m,B)(n,A)} - \frac{1}{i\omega L} V_{\downarrow,(m,B)(n,A)} - C(V_{\downarrow,(m,B)(n,B)} + V_{\downarrow,(m+1,A)(n,A)} + V_{\downarrow,(m+1,B)(n,A)}$$

$$+V_{\downarrow,(m,A)(n,A)} + V_{\downarrow,(m-1,B)(n,A)} + V_{\downarrow,(m,B)(n+1,A)} + V_{\downarrow,(m,B)(n-1,A)} + V_{\downarrow,(m,B)(n-1,B)}), \tag{S47}$$

$$\left(\frac{1}{i\omega L} - 2C\right) V_{\downarrow,(m,B)(n,B)} = 8C V_{\downarrow,(m,B)(n,B)} - C(V_{\downarrow,(m,B)(n+1,A)} + V_{\downarrow,(m,B)(n+1,B)}$$

$$+V_{\downarrow,(m,B)(n,A)} + V_{\downarrow,(m,B)(n-1,B)} + V_{\downarrow,(m+1,A)(n,B)} + V_{\downarrow,(m+1,B)(n,B)} + V_{\downarrow,(m,A)(n,B)} + V_{\downarrow,(m-1,B)(n,B)}). \tag{S48}$$

Combing Supplementary Eqs. (S37)-(S48), the eigen-equation of the designed electric circuit is described by

$$\left(\frac{f_0^{\,2}}{f^2} - 10\right) V_{\downarrow,(m,A)(n,A)} = -e^{-i\pi(\delta_{m,n} + \delta_{m,n+1})} \big(V_{\downarrow,(m,A)(n+1,A)} + V_{\downarrow,(m,A)(n,B)}\big)$$

$$-e^{i\pi(\delta_{m,n} + \delta_{m+1,n})} (V_{\downarrow,(m,A)(n-1,A)} + V_{\downarrow,(m,A)(n-1,B)}) - V_{\downarrow,(m,B)(n,A)} - V_{\downarrow,(m-1,B)(n,A)} - V_{\downarrow,(m+1,A)(n,A)}$$

$$-V_{\downarrow,(m-1,A)(n,A)} - \frac{C_P}{C} \delta_{m,n} (V_{\downarrow,(m,B)(n,B)} + V_{\downarrow,(m-1,B)(n-1,B)}) + \frac{C_V}{C} \delta_{m,n\pm1} V_{\downarrow,(m,A)(n,A)} + \frac{C_U + 2C_P}{C} \delta_{m,n} V_{\downarrow,(m,A)(n,A)}$$

(S49)

$$\left(\frac{f_0{}^2}{f^2}-10\right)V_{\downarrow,(m,A)(n,B)}=-e^{i\pi(\delta_{m,n})}V_{\downarrow,(m,A)(n,A)}-V_{\downarrow,(m+1,A)(n,B)}$$

$$-V_{\downarrow,(m-1,A)(n,B)}-V_{\downarrow,(m,B)(n,B)}-V_{\downarrow,(m-1,B)(n,B)}-V_{\downarrow,(n,A)(m-1,B)}-V_{\downarrow,(n,A)(m+1,A)}-V_{\downarrow,(n,A)(m+1,B)}, \quad \text{(S50)}$$

$$\left(\frac{f_0{}^2}{f^2}-10\right)V_{\downarrow,(m,B)(n,A)}=-e^{-i\pi(\delta_{m,n})}V_{\downarrow,(m,B)(n,B)}-V_{\downarrow,(m+1,A)(n,A)}-V_{\downarrow,(m+1,B)(n,A)}$$

$$-V_{\downarrow,(m,A)(n,A)}-V_{\downarrow,(m-1,B)(n,A)}-V_{\downarrow,(m,B)(n+1,A)}-V_{\downarrow,(m,B)(n-1,A)}-V_{\downarrow,(m,B)(n-1,B)}, \quad \text{(S51)}$$

$$\left(\frac{f_0{}^2}{f^2}-10\right)V_{\downarrow,(m,B)(n,B)}=-e^{-i\pi(\delta_{m,n}+\delta_{m,n+1})}\left(V_{\downarrow,(m,B)(n+1,A)}+V_{\downarrow,(m,B)(n+1,B)}\right)$$

$$-e^{i\pi(\delta_{m,n}+\delta_{m+1,n})}(V_{\downarrow,(m,B)(n,A)}+V_{\downarrow,(m,B)(n-1,B)})-V_{\downarrow,(m+1,A)(n,B)}-V_{\downarrow,(m+1,B)(n,B)}-V_{\downarrow,(m,A)(n,B)}$$

$$-V_{\downarrow,(m-1,B)(n,B)}-\frac{C_P}{C}\delta_{m,n}(V_{\downarrow,(m,A)(n,A)}+V_{\downarrow,(m+1,B)(n+1,B)})+\frac{C_U+2C_P}{C}\delta_{m,n}V_{\downarrow,(m,A)(n,A)}. \quad \text{(S52)}$$

We provide the following identification of tight-binding parameters in terms of circuit elements as

$$J=1, P=C_P/C, U=(C_U+2C_P)/C, V=C_V/C, f_0=1/2\pi\sqrt{LC}, \quad \text{(S53)}$$

where *J, P, U, V* and ε correspond to the strength of the particle hopping, the two-particle hopping, on-site interaction, nearest-site interaction and the eigen-energy of two anyons. In this case, Supplementary Eqs. (S49)-(S52) become

$$C_{(m,A)(n,A)} = -J(e^{i\theta(\delta_{m,n}+\delta_{m+1,n})}C_{(m,A)(n-1,A)}+e^{-i\theta(\delta_{m,n}+\delta_{m-1,n})}C_{(m,A)(n+1,A)}+C_{(m-1,A)(n,A)}+C_{(m+1,A)(n,A)}$$

$$+C_{(m,B)(n,A)}+e^{-i\theta(\delta_{m,n}+\delta_{m-1,n})}C_{(m,A)(n,B)}+C_{(m-1,B)(n,A)}+e^{i\theta(\delta_{m,n}+\delta_{m+1,n})}C_{(m,A)(n-1,B)})$$

$$-P\delta_{mn}(C_{(m,B)(n,B)}+C_{(m-1,B)(n-1,B)})+U\delta_{mn}C_{(m,A)(n,A)}+V\delta_{m(n\pm1)}C_{(m,A)(n,A)}, \quad \text{(S54)}$$

$$\varepsilon C_{(m,A)(n,B)} = -J(C_{(m,A)(n-1,B)}+C_{(m,A)(n+1,B)}+C_{(m-1,A)(n,B)}+C_{(m+1,A)(n,B)}$$

$$+e^{i\theta(\delta_{m,n}+\delta_{m+1,n})}C_{(m,A)(n,A)}+C_{(m,B)(n,B)}+C_{(m+1,A)(n,A)}+C_{(m,B)(n-1,B)}), \quad \text{(S55)}$$

$$\varepsilon C_{(m,B)(n,A)} = -J(C_{(m,B)(n-1,A)}+C_{(m,B)(n+1,A)}+C_{(m-1,B)(n,A)}+C_{(m+1,B)(n,A)}$$

$$+C_{(m,A)(n,A)}+e^{-i\theta(\delta_{m,n}+\delta_{m-1,n})}C_{(m,B)(n,B)}+C_{(m-1,B)(n,B)}+C_{(m,A)(n-1,A)}), \quad \text{(a56)}$$

$$\varepsilon C_{(m,B)(n,B)} = -J(e^{i\theta(\delta_{m,n}+\delta_{m+1,n})}C_{(m,B)(n-1,B)}+e^{-i\theta(\delta_{m,n}+\delta_{m-1,n})}C_{(m,B)(n+1,B)}+C_{(m-1,B)(n,B)}+C_{(m+1,B)(n,B)}$$

$$+e^{i\theta(\delta_{m,n}+\delta_{m+1,n})}C_{(m,B)(n,A)}+C_{(m,A)(n,B)}+e^{-i\theta(\delta_{m,n}+\delta_{m-1,n})}C_{(m+1,B)(n,A)}+C_{(m,A)(n+1,B)})$$

$$-P\delta_{mn}(C_{(m,A)(n,A)}+C_{(m+1,A)(n+1,A)})+U\delta_{mn}C_{(m,B)(n,B)}, \quad \text{(S57)}$$

with $C_{(m,\alpha)(n,\beta)}$ corresponding to $V_{\downarrow,(m,\alpha)(n,\beta)}$.

Note 6. Details on the fabricated circuit sample

We exploit the electric circuit by using PADs program software, where the PCB composition, stack up layout, internal layer and grounding designs are suitably engineered. Here, the well-designed PCB possesses totally six layers to arrange the intralayer and interlayer site-couplings. It is worth noting that the ground layer should be placed in the gap between any two layers to avoid their coupling. Moreover, all PCB traces have a relatively large width to reduce the parasitic inductance and the spacing between electronic devices is also large enough to avert spurious inductive coupling. The SMP connectors are welded on the PCB nodes for the signal input and detection. The tolerance of circuit elements and series resistance of inductors should be as low as possible. For this purpose, we use WK6500B impedance analyzer to select circuit elements with high accuracy (the disorder strength is only

1%) and low losses.

As for the measurement of the voltage evolution in the time-domain, we use the signal generator (NI PXI-5404) with eight output ports to act as the current source for exciting two circuit nodes related to a single lattice site with a constant amplitude and node-dependent initial phases. We measure the voltage signal at one circuit node. Generator (the initial phase is set to 0) is directly connected to one end of the oscilloscope (Agilent Technologies Infiniivision DSO7104B) to make sure an accurate start time. The measured voltage signals are in the range from 0ms to 5ms, where the 0ms is defined as the time for the simultaneously signal injection and measurement.

As shown in Figs. S3(a) and (b), we plot the photograph image of the fabricated circuit sample with $\theta = \pi$ and N=5. Enlarged views around the diagonal (enclosed by orange block) and far away from the diagonal (enclosed by the pink block) are plotted in Figs. S3(c) and (d).

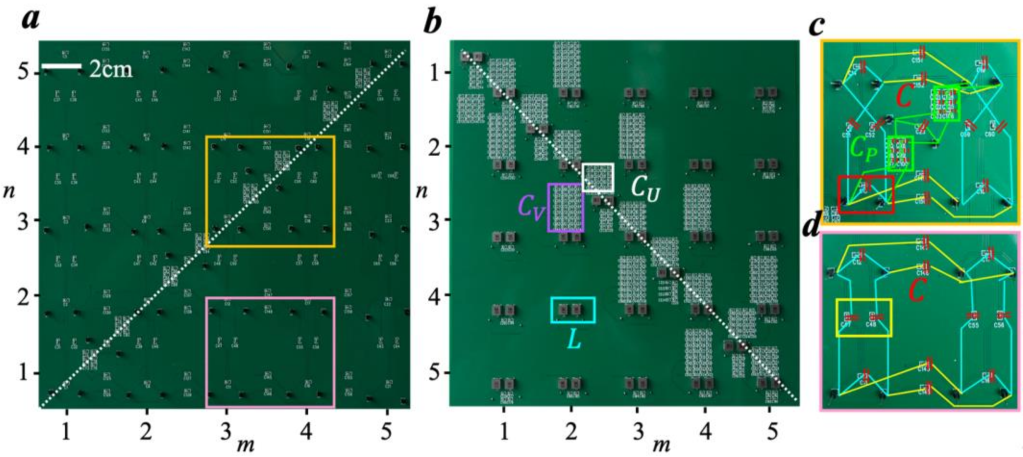

Fig. S3 (a) and **(b)** Photos of front and back sides for the fabricated 2D circuit with $\theta = \pi$ and N=5. Enlarged views around the diagonal (enclosed by orange block) and far away from the diagonal (enclosed by the pink block) are plotted in **(c)** and **(d)**.

Note 7. The influence of loss effect in the circuit sample

In this part, we evaluate the loss effect of the circuit. At first, we simulate the impedance spectrum of the (3,A),(3,A) node. Figs. S4(a)-(d) show the simulation results with the effective series resistances of inductance being 10 $m\Omega$, 50 $m\Omega$, 100 $m\Omega$ and 150 $m\Omega$, respectively. Similarly, Figs. S4(e)-(h) and Figs. S4(i)-(l) present simulated impedance spectra of the (4,A),(2,A) and (1,A),(1,A) nodes with the same values for the effective series resistances of inductance used in Figs. S2(a)-(d). We can see that the larger the loss value is, the lower the impedance peak (the larger the impedance peak width) becomes. Comparing with the experimental results in Fig. 3 of the main text, it can be seen that the effective loss in our circuit sample is about 100 $m\Omega$.

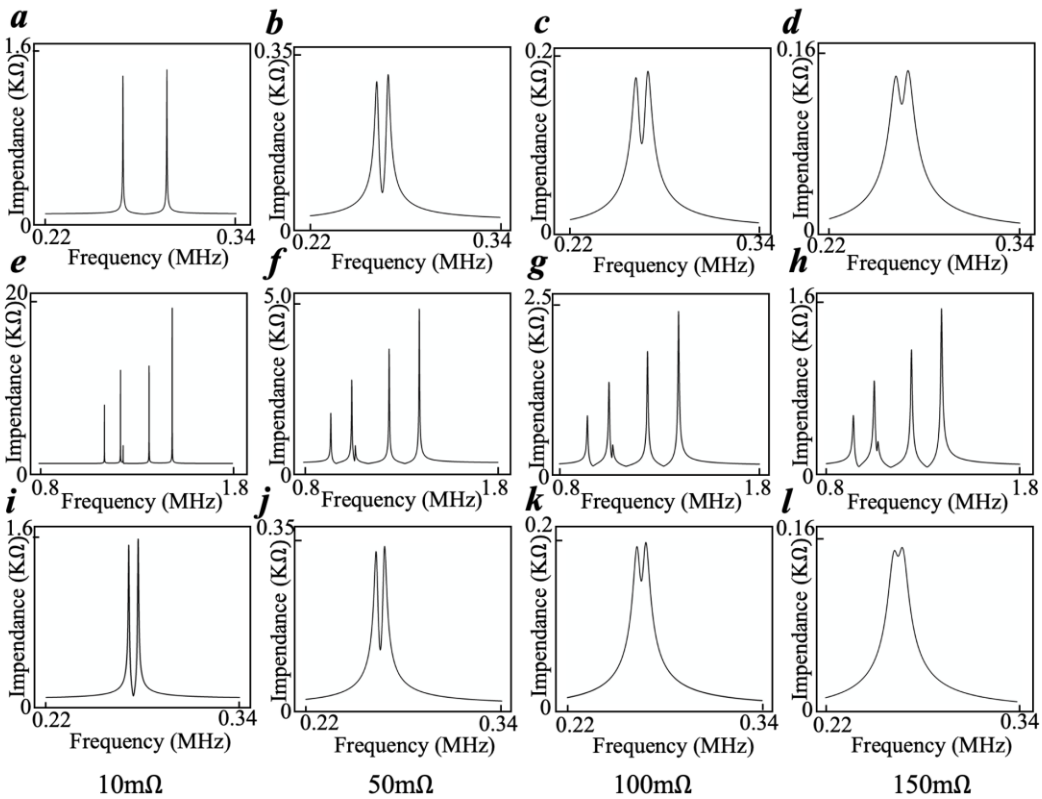

Fig. S4 (a-d) Simulated impedance responses of the (3,A)(3,A) node with the effective series resistance of inductance being 10 $m\Omega$, 50$m\Omega$, 100$m\Omega$ and 150$m\Omega$, respectively. **(c-h)** Simulated impedance responses of the (4,A)(2,A) node with the effective series resistance of inductance being 10 $m\Omega$, 50$m\Omega$, 100$m\Omega$ and 150$m\Omega$, respectively. **(i-l)** Simulated impedance responses of the (1,A)(1,A) node with the effective series resistance of inductance being 10 $m\Omega$, 50$m\Omega$, 100$m\Omega$ and 150$m\Omega$, respectively.

Note 8. Numerical results of impedance responses in electric circuits with different effective statistical angles

In this part, we introduce the simulation method on tuning the effective statistical angle of two anyon in electric circuits, and theoretically investigate the influence of effective statistical angle on the formation of topological flatbands in electric circuits by impedance measurements and voltage dynamics, that is, the proposition that the topological transition caused by a certain parameter should be included in our experimental design, and the topological sequence parameter is adjustable and can be visualized.

As shown in Fig. S5(a), the schematic diagrams on the realization of different valued effective statistical angle in electric circuits with $\theta = \pi$, 0.8π, $2/3\pi$, 0.5π and 0 are presented. We note that the eigenequations of electric circuits with different values of the effective statistical angle are consistent to eigenequation of two anyons with different statistical angles. Then, we calculate the impedance responses at $\{(3,B),(3,B)\}$ node in these circuits, as shown in Fig. S5(b). It is clearly shown that there is always a large central impedance peak at 0.2656Hz and the frequency of such impedance peak is matched to the eigenenergy of two-anyon flat band at ε =102.8. These results are consistent with our theoretical model that there is always a statistical angle-independent two-anyon flat band at $\varepsilon = 102.8$. In addition, lots of impedance peaks appear at two sides of the central impedance peak with the low-value of θ, manifesting the significant dispersion effect of high-energy and low-energy two-anyon bands. By increasing the value of effective statistical angle, the peak number is decreased and impedance value is increased, consisting to the flat-band properties. These results clearly shown that our designed electric circuits can simulate the effective statistical angles induced anyonic flat bands.

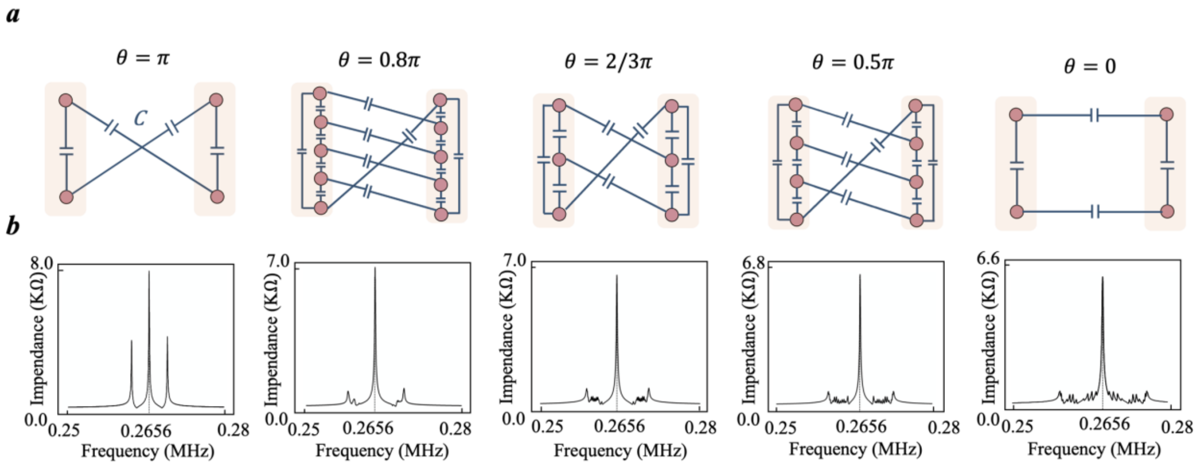

Fig. S5 (a) The schematic diagrams on the realization of different-valued effective statistical angle by electric circuits. **(b)** Numerical results of the impedance responses of designed electric circuits with different effective statistical angles of $\theta = \pi$, 0.8π, $2/3\pi$, 0.5π and 0.

Note 9. Simulation results of voltage dynamics

In this part, we simulate the voltage dynamics. Here, the circuit excitation is in the form of $[V_1 = V_0 e^{i\omega t}, V_2 = -V_0 e^{i\omega t}]$. In order to avoid the influence of size, the simulated circuit side is set to 16×16 nodes, and the corresponding parameters are the same to that used in Fig. 4 (in the main text). Firstly, to simulate the localization phenomenon caused by the two-anyon flat band effect, we input the voltage signal at the (11,A),(11,A) node. The associated excitation frequency is set as 0.269MHz, which matches to the two-anyon flat-band bulk mode. Fig. S6(a) shows the voltage signal in the time range from 0 to $5ms$. In addition, we plot the voltage distribution at $3ms$, as shown in Fig. S6(b). We can clearly see that in the clean circuit, the extremely high voltage signal concentrates at several circuit nodes near the excitation point. Then, we simulate the voltage evolution by exciting the (14,A),(2,A) circuit node at frequency 0.139MHz (matched to the two-anyon scattering states), as shown in Fig. S6(c). Fig. S6(d) displays the corresponding spatial profile of voltage signal at $3ms$. It is clearly shown that the input voltage signal quickly diffuses into the whole space over time, indicating that there is no dynamic localization phenomenon. Finally, we input the voltage signal at the (1,A)(1,A) node to simulate the voltage dynamics related to two-anyon topological edge states, as shown in Fig. S6(e). The associated excitation frequency is set as 0.263MHz, which matches to the two-anyon topological edge mode. Fig. S6(f) plots the distribution of the voltage signal at $3ms$. We can see that the extremely high voltage signal concentrates at circuit nodes of (1,A),(1,A) and (1,B),(1,B). Similar to the experimental results, those results clearly demonstrate the existence of topological edge states.

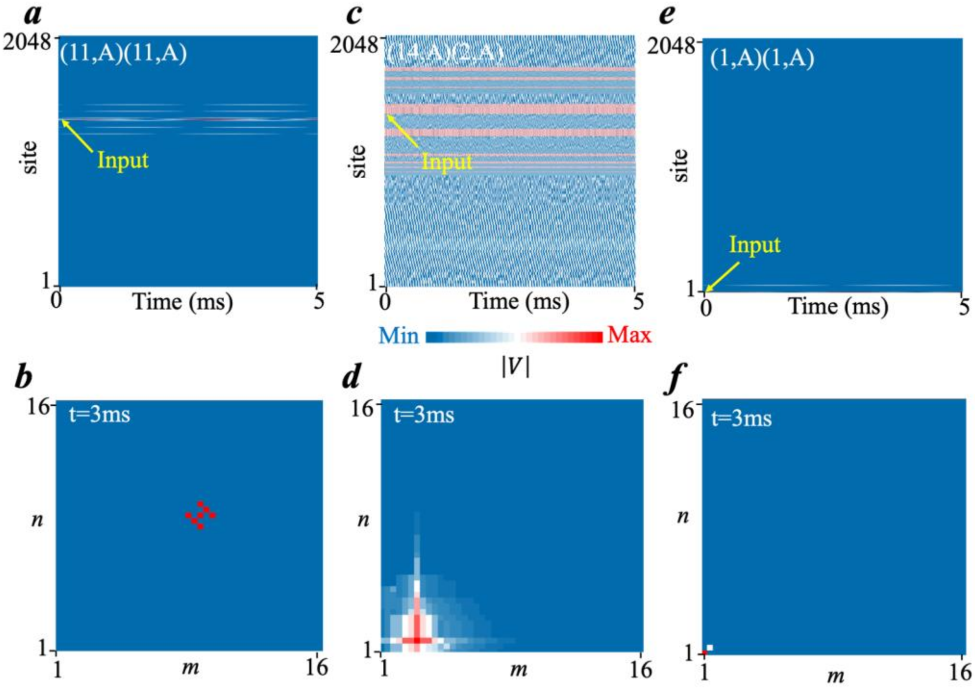

Fig. S6 (a), (c) and **(e)** The simulation results of the time dynamics of (11,A)(11,A), (14,A)(2,A) and (1,A)(1,A) nodes. **(b), (d)** and **(f)** The distribution of the voltage amplitude at t=3*ms* related to results in Figs. S6 (a), (c) and (e), respectively.